ACS Sustainable Chemistry & Engineering

pubs.acs.org/journal/ascecg

Research Article

Bio-Based Nanofluids of Extraordinary Stability and Enhanced Thermal Conductivity as Sustainable Green Heat Transfer Media

Karolina Brzóska,* Adrian Golba, Michał Kuczak, Anna Mrozek-Wilczkiewicz, Sławomir Boncel,* and Marzena Dzida*

Cite This: *ACS Sustainable Chem. Eng.* 2021, 9, 7369–7378

Read Online

ACCESS | Metrics & More | Article Recommendations | Supporting Information

ABSTRACT: Nanofluids (NFs) as a new generation of heat transfer media can be applied inter alia as engine coolants, in the microelectronic industry for the cooling of electronic components and systems, and in solar panels. In the present study, the extraordinarily, that is, more than 1 year, stable NFs composed of multi-walled carbon nanotubes (MWCNTs), biomass-derived 1,2-propanediol or 1,3-propanediol, and poly(*N*-vinylpyrrolidone) were created and studied. The thermal conductivity and density of NFs did not change over 8 months, and NFs did not sediment over 14 months. The real image of NFs determined using transmission electron cryo-microscopy allowed us to prove that the extraordinary stability and enhanced thermal conductivity were resulted by fully individualized MWCNTs in the continuous phase and MWCNTs stabilized in dispersions by shorter carbon nanoparticles and mostly homogenous poly(*N*-vinylpyrrolidone) coating. The maximum enhancement in thermal conductivity was 22 and 20% for NFs composed of 2 wt % MWCNTs in comparison with that of pure 1,2-propanediol and 1,3-propanediol, respectively. The improved thermal properties were accompanied by the practically Newtonian nature of all NFs. The cytotoxicity test on normal human dermal fibroblasts indicated that the use of diols diminished the toxicity of MWCNTs. Finally, the thermal conductivity and Prandtl number of bio-based NFs—as compared with those of commercial heat transfer fluids DOWCAL 200 and DOWCAL N—predestine them as superb green heat transfer media in sustainable energy systems.

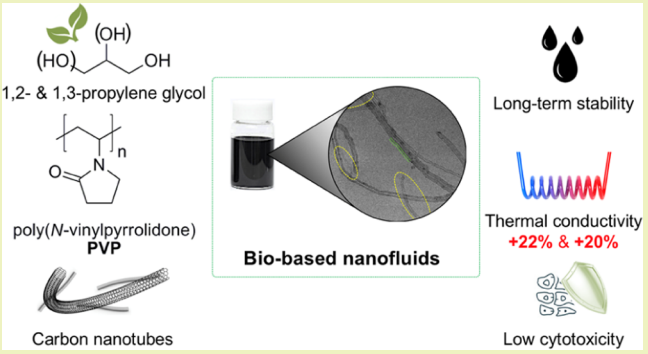

KEYWORDS: *nanofluids, 1,2-propanediol, 1,3-propanediol, multi-walled carbon nanotubes, thermal conductivity, green media, heat transfer fluids*

INTRODUCTION

The obligation to limit the current consumption of fossil fuels necessitates the use of alternative, greener energy sources which improve the efficiency and effectiveness of the heat exchange devices. The most commonly used heat transfer medium is water. In turn, in refrigeration, thermal systems operating in cold regions, car radiators, or industrial heat exchangers, the aqueous mixtures of 1,2-ethanediol (EG) are used in order to lower the freezing point and elevate the boiling point of working heat transfer fluids (HTFs). However, EG is produced mainly from fossil fuels. Thus, the alternative base liquids obtained from renewable feedstock should be considered. 1,2-Propanediol (1,2-PG) and 1,3-propanediol (1,3-PG) are more suitable base liquids than EG. 1,2-PG used in this work is produced from waste glycerin from the production of biodiesel from vegetable oils.[1] In turn, 1,3-PG is produced from plants or also from glycerin.[2] Susterra 1,3-PG used in this work is produced from corn cobs.[3] The benefits of using bio-based 1,2-PG and 1,3-PG include reduction in the energy expenditure and greenhouse gas emissions as compared to that in the production of glycols from petrochemical raw materials. In addition to the green chemistry aspect, these are sustainable products with a low carbon footprint and a wide industrial use. Their production is characterized by a 50% reduction in CO_2 emission when compared to that in the fossil processing.[4] Susterra 1,3-PG, of a "cradle-to-grave" life cycle, generates up to 56% less emission of greenhouse gases and consumes 42% less non-renewable energy than the petroleum-based 1,3-PG.[5] In addition, PGs are characterized by low freezing temperature, non-toxicity, and faster biodegradation than EG.[6] The toxicity of EG surpasses that of 1,3-PG considering lethality, acute effects, and reproductive, developmental, and kidney toxicity.[7] 1,3-PG is characterized by

Received: March 21, 2021
Revised: May 4, 2021
Published: May 18, 2021

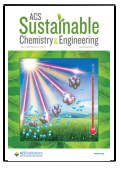

decomposition at higher temperatures[5] and hence displays the enhanced operational stability as an HTF. However, the thermal conductivity of EG and PGs is about 2 and 3 times lower than that of water at 20 °C, respectively. Nevertheless, this limitation may be overcome by employing nanofluids (NFs) which constitute a prospective solution in the design and manufacture of the modern HTFs. The most intensively studied carbon nanotube-based NFs are based on EG[8,9] and, recently, on ionic liquids.[10,11] Although 1,2-PG and 1,3-PG have many advantages, multi-walled carbon nanotube (MWCNT)-based NFs with propanediols as base fluids are rarely investigated.[6,12] Boncel et al.[12] found that 1,3-PG-based NFs containing 0.53 vol % curly ultra-long MWCNTs, stabilized with gum arabic in water, emerged as 39% more heat-conducting than pristine 1,3-PG. Nevertheless, the rheological characteristics and NF stability at high MWCNT concentrations were not cross-verified. Generally, in order to improve the dispersion stability in the base liquid, nanoparticle (NP) stabilizers are used. Poly(*N*-vinylpyrrolidone) (PVP) is often used as a stabilizer for NFs composed of metal NPs, but it has not been studied deeply as a stabilizer for MWCNT-based NFs so far. For the industrial applications where HTFs work in flow regimes, the viscosity of the HTFs directly impacts the pressure drop and, as a consequence, the required pumping power to transport them. However, most of the literature studies to date have mainly focused on the heat transfer part; few have provided reliable data on the viscosity of NFs.[6] For instance, Mary et al.[13] conducted comprehensive research including thermal conductivity, viscosity, and colloidal and thermal stability. They found the reproducibility of thermal conductivity of NFs composed of 0.1, 0.2, 0.3, and 0.5 vol % MWCNTs and 1,3-PG after 15 days as an indicator of colloidal stability of the dispersions. Moreover, they examined viscosity and high temperature stability. The studied NFs maintained the shear-thinning behavior and colloidal stability even at temperatures as high as 140 °C.

Taking into consideration all the above facts, in this work, we study the bio-based NFs composed of 1,2-PG or 1,3-PG as base liquids derived from biomass, non-toxic PVP, and short MWCNTs, which are safe as immobilized/non-inhalable particles in liquids and biodegradable by enzymes, for example, peroxidases.[14−17] We have examined the long-term stability under different temperature conditions (24 and 70 °C) by visual observation of sedimentation and additionally using centrifugation at various rotational speeds. Also, we have measured the thermal conductivity and density of NFs immediately after preparation and 8 months after preparation. The improved stability and thermophysical properties were confirmed by a real image of the NFs obtained by means of transmission electron cryo-microscopy (cryo-TEM). For the comprehensive characterization, we have studied isobaric heat capacity as well as viscosity as a function of the temperature and shear rate in order to examine the Newtonian behavior of NFs. Additionally, the cytotoxicity on normal human dermal fibroblasts has been examined. The thermal conductivity and Prandtl number of studied NFs were compared with those of the commercial HTFs DOWCAL 200 and DOWCAL N, which has revealed superb characteristics of the herein proposed systems.

MATERIALS AND METHODS

Materials. MWCNTs were purchased from Nanostructured & Amorphous Materials, Inc., Katy, USA. Pristine as-purchased MWCNTs were characterized using scanning electron microscopy (SEM) (Figure 1A) and transmission electron microscopy (TEM)

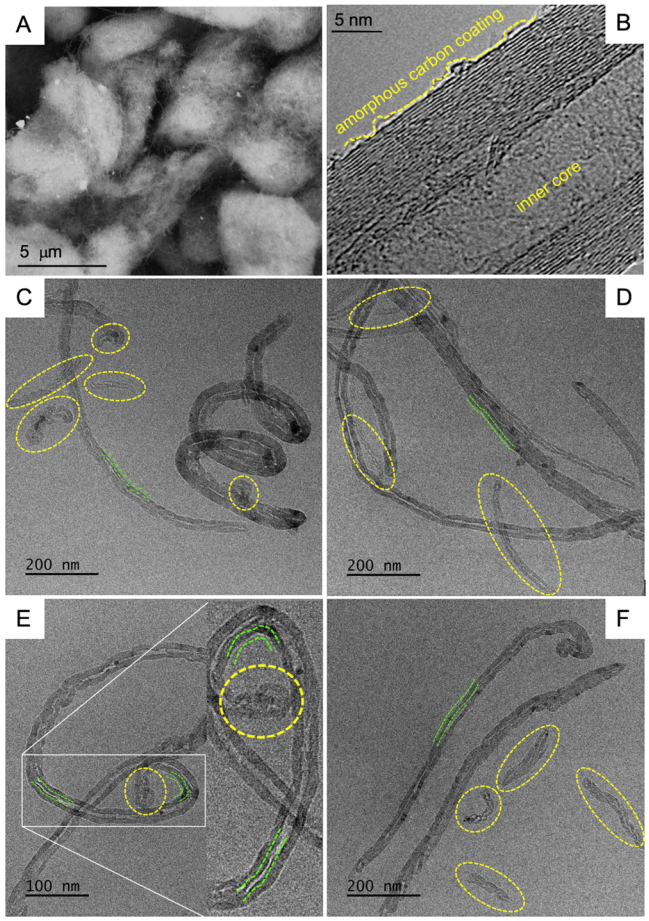

Figure 1. SEM (A) and TEM (B) images of pristine MWCNTs. Cryo-TEM images of PVP-coated MWCNTs in 1,2-PG (C,D) and 1,3-PG (E,F, magnified inset in E). The yellow ellipses indicate smaller nanotubes and/or amorphous carbon, while light-green tracks show PVP coating.

(Figure 1B). The sub-micron morphology of MWCNTs was determined by TEM imaging [analysis program and a CCD (Eagle 4K) camera]. The TEM micrographs were acquired using a Tecnai G2 F20 TWIN electron microscope at a bias voltage of 200 kV. The surface morphology of MWCNTs was studied by means of a Phenom Pro-X scanning electron microscope operating at 10 kV. SEM analysis revealed that, at the microscale, MWCNTs formed clusters of highly entangled individual quasi-one-dimensional (1D) few micron-long fibrils. The nanotube bundles contained a few catalyst and catalyst-support nanoparticles of sizes from ca. 50 to 400 nm, visible as irregular, brighter spots. At the same time, TEM images revealed that the individual nanotubes were composed of a few to a few dozen walls, typically more graphitized upon approaching the nanotube inner core. The specifications of MWCNTs are presented in Table 1.

PVP was supplied by Sigma-Aldrich. 1,2-PG was purchased from Oleon Company. 1,3-PG was purchased from DuPont Tate & Lyle Bio Products Company. All the samples were dried before the experiment using 4 Å molecular sieves (Merck, Germany). The water content was determined using the Karl Fischer method (Metrohm 870KF Titrino Plus). Brief specifications of propanediols are presented in Table 2. The density, viscosity, and thermal conductivity obtained in this work are in very good agreement with the literature data,[18−26] that is, the relative deviations are lower than the declared uncertainty of the measurements (see Table S1 in the Supporting Information).

https://doi.org/10.1021/acssuschemeng.1c01944
ACS Sustainable Chem. Eng. 2021, 9, 7369−7378

Table 1. MWCNT Specification

nanoparticles	purity (wt %)	density ($g \cdot cm^{-3}$)	specific surface area ($m^2 \cdot g^{-1}$)	OD[a] (nm)	ID[b] (nm)	length (μm)
MWCNTs	>95	2.1	>40	50−80	5−15	0.5−2

[a]Outer diameter. [b]Inner diameter.

Table 2. Name, Acronym, CAS Number, Purity, and Water Content of Propanediols

name	acronym	CAS number	purity (wt %)[a]	water content (ppm)[b]
1,2-propanediol	1,2-PG	57-55-6	99.9	260
1,3-propanediol	1,3-PG	504-63-2	99.7	240

[a]Declared by supplier. [b]Karl Fischer method (Metrohm 870KF Titrino Plus).

Sample Preparation. The NFs were prepared by a tree-step method. First, PVP was added to the base fluids. Then, the proper mass of MWCNTs (0.5, 1.0, 1.5, and 2.0 wt %) was added, and the dispersions were mixed using a magnetic stirrer at 600 rpm for 10 min (Wigo MS11, Poland). Finally, the samples were sonicated using a 200 W UP200Ht homogenizer with a sonotrode of diameter 15 mm (Hielscher, Germany). The ice bath was used to prevent the overheating of dispersions. The energy supplied to each sample during the sonication was equal to 0.16 W $h \cdot g^{-1}$.

Stability Investigations. The stability was tested at 24 ± 2 and at 70 ± 0.1 °C using a laboratory oven (Memmert, Germany) and centrifugation at various rotational speeds ranging from 800 to 13400 rpm (MiniSpin Eppendorf centrifuge). The tested systems were weighed on an analytical balance (Acculab ATL-224-V, Sartorius Group) with an accuracy of 0.0001 g. On the basis of the determined density, 1.4 mL each of the samples was weighed.

Cryo-TEM Measurements. The cryo-TEM images were obtained using a Tecnai F20 X-TWIN microscope (FEI Company, Hillsboro, Oregon, USA) equipped with a field emission gun, operating at an acceleration voltage of 200 kV. Images were recorded on a Gatan Rio 16 CMOS 4k camera (Gatan Inc., Pleasanton, California, USA) and processed with Gatan Microscopy Suite (GMS) software (Gatan Inc., Pleasanton, California, USA). Specimen preparation was done by vitrification of the aqueous solutions on grids with a holey carbon film (Quantifoil R 2/2; Quantifoil Micro Tools GmbH, Großlöbichau, Germany). Prior to use, the grids were activated for 15 s in oxygen plasma using a Femto plasma cleaner (Diener Electronic, Ebhausen, Germany). Cryo-samples were prepared by applying a droplet (3 μL) of the suspension to the grid, blotting with filter paper, and immediately freezing in liquid ethane using a fully automated blotting device, Vitrobot Mark IV (Thermo Fisher Scientific, Waltham, Massachusetts, USA). After preparation, the vitrified specimens were kept under liquid nitrogen until they were inserted into a cryo-TEM holder, Gatan 626 (Gatan Inc., Pleasanton, USA), and analyzed in the transmission electron microscope at −178 °C.

Density Measurements. The density of pure diols and NFs was measured using Anton Paar DMA 5000M and Anton Paar DMA 5000 vibrating tube densitometers with the automatic viscosity correction and expanded measurement uncertainties of $\pm 5 \times 10^{-2}$ and $\pm 3 \times 10^{-1}$ $kg \cdot m^{-3}$, respectively. The temperature was measured with an expanded uncertainty of ±0.02 °C.

Thermal Conductivity Measurements. The thermal conductivity of base fluids and NFs was measured using the Thermtest Transient Hot Wire (THW-L2) liquid thermal conductivity meter via the hot-wire technique according to the standard ASTM D 7896-19.[27] The hot-wire method is a technique based on the measurement of the temperature rise at a defined distance from a linear heat source (hot wire—60 mm in length) embedded in the test material. A constant current source heats the sensor wire, while this pulse generates a temperature field in the shape of cylindrical concentric isothermal surfaces. The temperature of the samples was maintained by a thermostatic air bath with a stability of ±0.1 °C. Before the measurement, the instrument was calibrated using deionized ultra-filtered water as a reference standard (2.0 $\mu\Omega \cdot cm^{-1}$; 0.6065 $W \cdot m^{-1} \cdot K^{-1}$ at 25 °C).[28] The reference standards were glycerin anhydrous (Fluka, mass fraction purity of 0.995, water content 150 ppm), toluene (POCH, mass fraction purity of 0.995, water content 200 ppm), and *n*-heptane (Merck, mass fraction purity of 0.995, water content 27 ppm). The apparatus was also tested using 2-propanol (Sigma-Aldrich, mass fraction purity of 0.999, water content 230 ppm), anhydrous 1-butanol (Sigma-Aldrich, mass fraction purity of 0.998, water content 260 ppm), and EG (Fluka, mass fraction purity of 0.995, water content 190 ppm). The differences between the thermal conductivity obtained in this work and reference standards equal 0.0% for glycerin;[29] 0.10% for toluene;[30] 0.16% for *n*-heptane;[31] 3.1[32] and −2.2% for 2-propanol;[24] 3.4,[32] 0.0%,[24] and −0.33% for 1-butanol;[33] and 2.0[34] and 0.0%[22,35] for EG (see Table S2 in the Supporting Information). The uncertainty of the thermal conductivity measurements was estimated to be ±5%.

Viscosity Measurements. Rheological properties of NFs were collected using the rotary viscometer LV DV2T (Brookfield Engineering, USA) with a small sample adapter and a SC4-18 spindle. The temperature was controlled with a low-profile refrigerated circulator (PolyScience MX7LR-20, USA) containing an EG−water system. The temperature stability of the circulator was ±0.07 °C. The uncertainty of viscosity measurements was ±3 mPa·s. The MCR 302 rheometer (Anton Paar, Germany) with the plate−plate system CP50-1 was used to measure the viscosity as a function of the shear rate at 25 °C. Temperature stability was maintained by means of a Peltier system at 0.01 °C. The viscosity of pure diols was measured with a ViscoClock viscometer (SI Analitics, Germany) and Ubbelohde capillaries with constants $K = 0.09740$, $K = 0.2934$, and $K = 0.9510$ (SI Analytics, Germany). The accuracy of time measurement equaled ±0.01 s. A CT 72/2-TT bath (SI Analytics, Germany) was used to stabilize the temperature, and the temperature stability was ±0.01 °C. The uncertainty of viscosity measurements was ±1%.

Isobaric Heat Capacity Measurements. The isobaric heat capacity was measured using a differential temperature scanning microcalorimeter μSC−2c (SETARAM). The apparatus was calibrated based on the Joule effect. The reference standard was 1-butanol (Sigma-Aldrich, SureSeal, anhydrous, mass fraction purity of 0.998). The apparatus was tested using *n*-hexane (POCH, Poland, mass fraction purity of 0.999) and benzene (Sigma-Aldrich, mass fraction purity of 0.998). The expanded uncertainty of the isobaric heat capacity measurements was equal to ±2%.

Cytotoxicity Studies. The normal human dermal fibroblast cell line NHDF (normal human dermal fibroblast) was purchased from PromoCell. The cells were grown as monolayer cultures in 75 cm^2 flasks (Nunc) in Dulbecco's modified Eagle's medium (DMEM). The DMEM was supplemented with 15% non-inactivated fetal bovine serum (FBS, Sigma) and 1% v/v penicillin/streptomycin (Gibco). The cells were cultured under standard conditions at 37 °C in a humidified atmosphere at 5% CO_2. The cell line was tested for mycoplasma contamination using the polymerase chain reaction technique. The tested 1,2-PG and 1,3-PG samples were dissolved in the culture medium to achieve the necessary concentrations. Four milligrams of NFs composed of 2 wt % MWCNTs and 1,2-PG or 1,3-PG was dispersed in an FBS-free medium containing bovine serum albumin (BSA) at a final concentration of 0.5 mg/mL and sonicated for 1 min. The exponentially growing cells were harvested through the trypsinization of sub-confluent cultures. The cells were seeded onto 96-well plates (Nunc) at a concentration of 4000 cells/well and incubated at 37 °C for 24 h. After this time, the growth medium was exchanged for a medium containing the tested materials at various concentrations. The cells were incubated with the materials for 72 h under standard cell culture conditions. Then, the medium was

https://doi.org/10.1021/acssuschemeng.1c01944
ACS Sustainable Chem. Eng. 2021, 9, 7369−7378

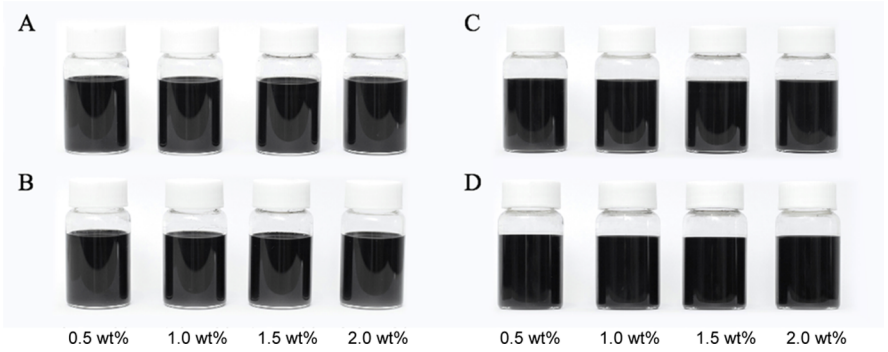

Figure 2. Photographs of NFs composed of MWCNTs + 1,2-PG (A) immediately after sonication and (B) 14 months after preparation. Photographs of NFs composed of MWCNTs + 1,3-PG (C) immediately after sonication and (D) 14 months after preparation. (B,D) The pictures are the same for samples stored at 24 and 70 °C.

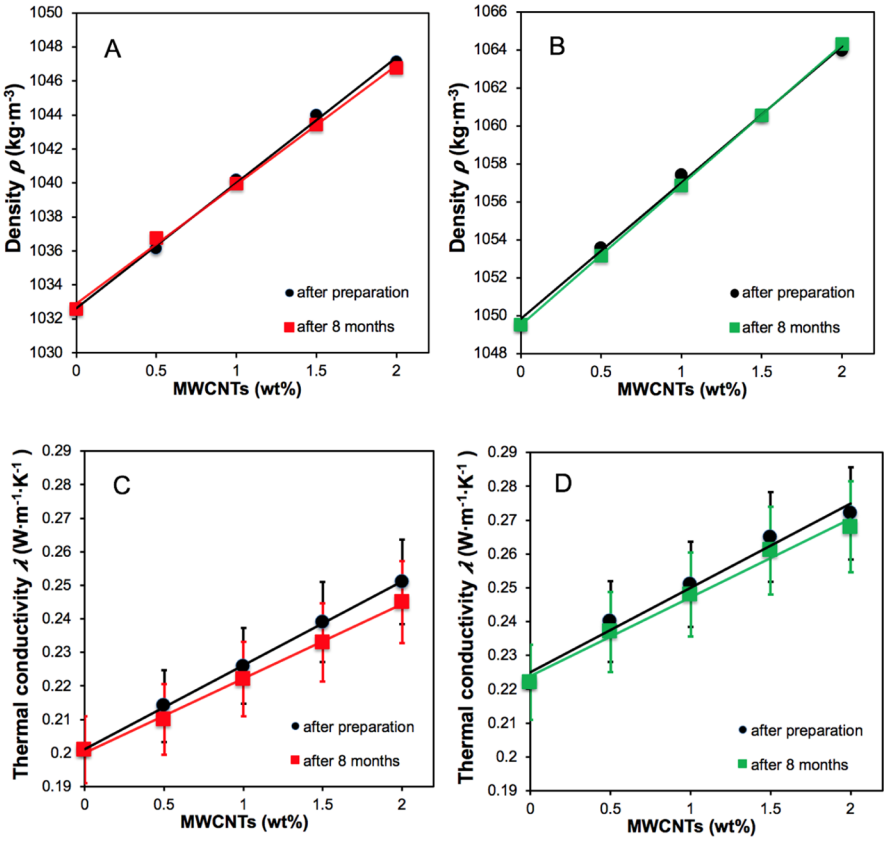

Figure 3. Density of stable NFs composed of (A) MWCNTs + 1,2-PG and (B) MWCNTs + 1,3-PG, measurements after sonication and 8 months after preparation at 25 °C. Thermal conductivity of stable NFs composed of (C) MWCNTs + 1,2-PG and (D) MWCNTs + 1,3-PG, measurements after sonication and 8 months after preparation at 25 °C.

replaced with 100 μL of DMEM without Phenol Red. The metabolic activity of viable cells was determined by adding 20 μL of CellTiter 96AQueousOne Solution—methyl tetrazolium salt (MTS) [3-(4,5-dimethylthiazol-2-yl)-5-(3-carboxymethoxyphenyl)-2-(4-sulfophenyl)-2*H*-tetrazolium, inner salt] (Promega)—followed by 1 h incubation. The MTS assay as a colorimetric method was used for determining the number of viable cells. Here, a standard solution containing 100 μL of DMEM without Phenol Red and 20 μL of the MTS solution was applied to determine the "blank" absorbance. The cell viability was calculated as a percent compared to untreated cells (control) and presented as mean values with standard deviation. Each compound was individually tested in triplicate in a single experiment, while each experiment was repeated four times.

RESULTS AND DISCUSSION

The usefulness and the possibility of industrial applications of NFs depend mainly on the dispersibility of NPs in the base fluids and stability of so-formed NFs over time and under various operating conditions. The stability of NFs is typically understood as no sedimentation and no aggregation of NPs, as well as no change in the physicochemical parameters in the range of measurement uncertainty. Concerning the analysis of the dispersed phase of NFs, one might clearly observe via cryo-TEM imaging (Figure 1C−F), at the lower magnification, fully individualized MWCNTs in the continuous phase. MWCNTs were found as curly objects up to 2 μm in length. It should be emphasized that, upon the treatment via the elaborated

https://doi.org/10.1021/acssuschemeng.1c01944
ACS Sustainable Chem. Eng. 2021, 9, 7369−7378

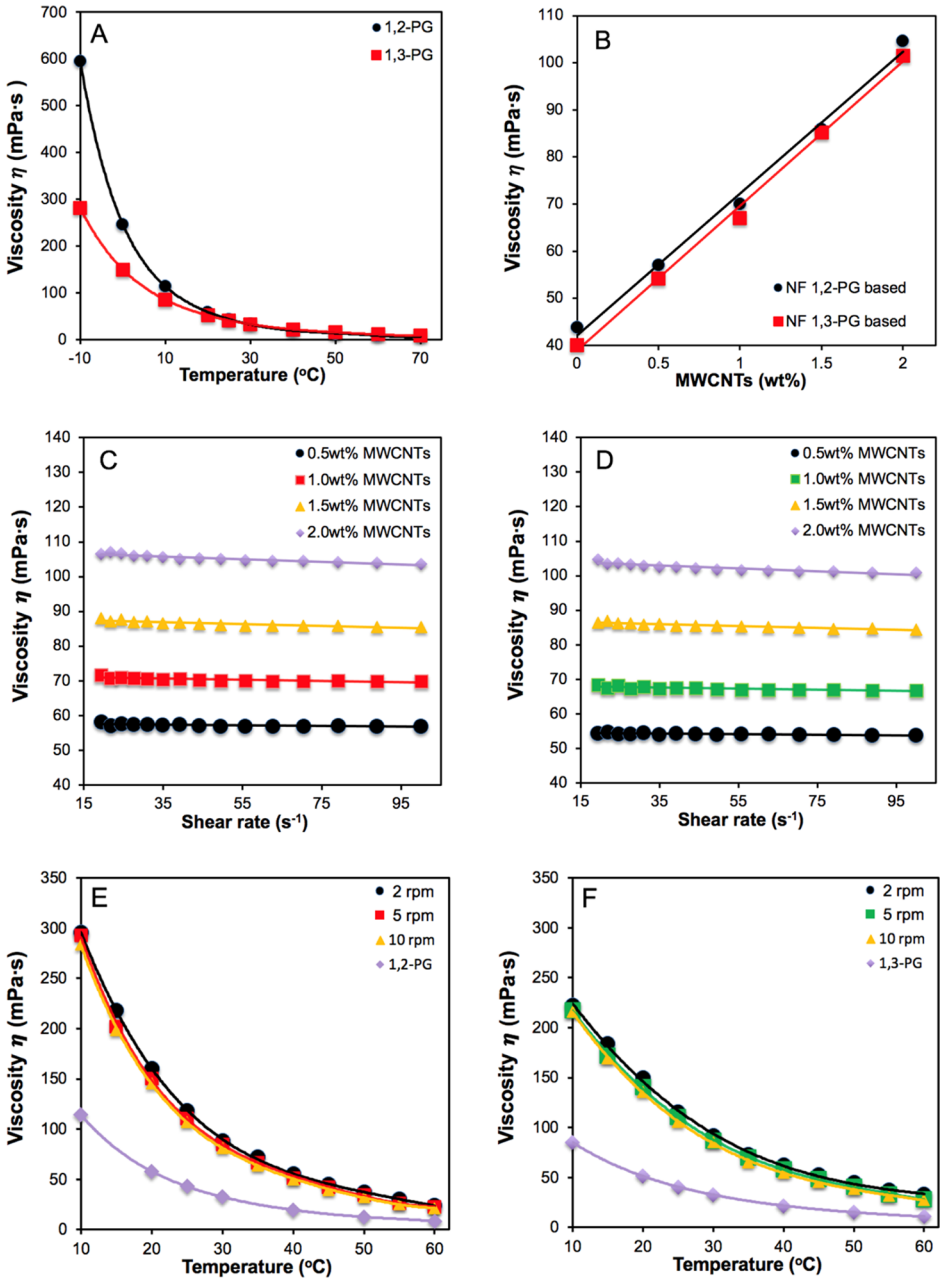

Figure 4. Rheological characteristics of the studied systems: (A) temperature dependence of the viscosity of pure 1,2-PG and 1,3-PG. (B) Viscosity as a function of the MWCNT concentration of stable NFs composed of MWCNTs + 1,2-PG and MWCNTs + 1,3-PG at 25 °C and at a shear rate of 62.6 s^{-1}. Viscosity as a function of the shear rate of stable NFs composed of (C) MWCNTs + 1,2-PG and (D) MWCNTs + 1,3-PG at 25 °C. Comparison of the temperature dependence of viscosity of (E) pure 1,2-PG and stable NFs composed of 2 wt % MWCNTs + 1,2-PG; (F) pure 1,3-PG and stable NFs composed of 2 wt % MWCNTs + 1,3-PG.

protocol, MWCNTs could be stabilized in dispersions by shorter nanotubes or amorphous elongated/ellipsoidal or spheroidal carbon nanoparticles[36,37] as well as by mostly homogenous PVP coating,[38] as indicated by yellow dashed line regions and light-green tracks, respectively. It must be emphasized that the enhanced stability, if achieved, should not only yield prolonged operational performance but also lead to the development of a three-dimensional network of MWCNTs interconnected by thermal bridges, again composed of MWCNTs of various lengths. Such stability of the NFs was monitored by their visual observation in tightly sealed laboratory bottles. For all NFs, no sedimentation was observed at 24 ± 2 and 70 ± 0.1 °C for 14 months (Figure 2).

The stability of NFs was also tested by centrifugation at various rotational speeds ranging from 800 to 13,000 rpm in the 15 min period. The NFs were centrifuged at speeds in the range 2000−8000 rpm in steps of 1000 rpm and additionally at 13,000 rpm. For NFs based on 1,2-PG, the sedimentation was observed at 5000 rpm. At higher centrifugation speeds (6000−8000 rpm), no changes were observed. At 13,000 rpm, larger amounts of the precipitate were detected. It may indicate that some amounts of MWCNTs were not dispersed properly or aggregated under the high centrifugation speed. For NFs based on 1,3-PG at 2000 rpm and 3000 rpm, no sedimentation was observed. At higher centrifugation speeds (4000−8000 rpm), a higher wettability of the Eppendorf tube walls by NFs based on

https://doi.org/10.1021/acssuschemeng.1c01944
ACS Sustainable Chem. Eng. 2021, 9, 7369−7378

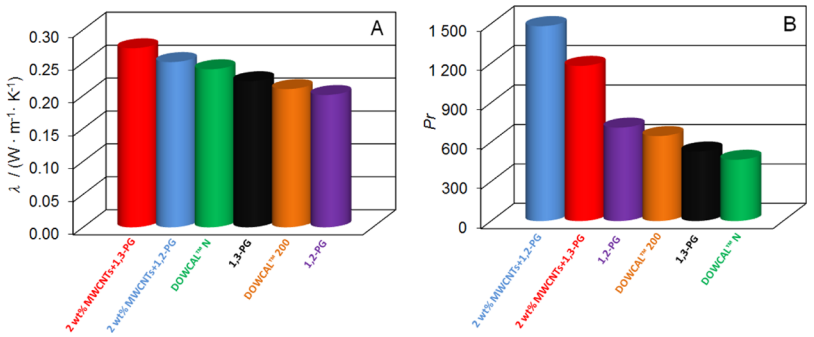

Figure 5. Comparison of (A) thermal conductivity and (B) Prandtl number of NFs, pure diols, and commercial HTFs DOWCAL 200 or DOWCAL N at 20 °C.

1,3-PG was observed, regardless of the MWCNT concentration. At 5 days after centrifugation at 13,000 rpm, a small amount of the precipitate at the bottom of the test tube was observed, which may indicate sedimentation of MWCNTs. The stability of the examined systems was also confirmed by density measurements. The density of the NFs was measured in the temperature range from 5 to 90 °C immediately after sonication and 8 months after sample preparation at 25 °C. The experimental results are collected in the Supporting Information in Tables S3−S6. After 8 months, density differences did not exceed −0.06 and 0.04% at 25 °C for 1,2-PG-based and 1,3-PG-based NFs, respectively (see also Figure 3A,B and Tables S4 and S6).

The main idea of the nano-additives is to increase the conductivity of NFs. The thermal conductivity of the NFs was measured at 25 and 70 °C immediately after sonication and at 25 °C 8 months after the sample preparation. The experimental results for 1,2-PG-based or 1,3-PG-based NFs are collected in Tables S7 and S8, respectively, in the Supporting Information. The addition of MWCNTs—as the thermoactive dispersed quasi-1D phase—remarkably improved the thermal conductivity of NFs. The maximum enhancement in thermal conductivity was 22 and 20% for NFs composed of 2 wt % MWCNTs in comparison with that of pure 1,2-PG and 1,3-PG, respectively. As found, the thermal conductivity was temperature-independent. What is also important, 8 months after the sample preparation, the thermal conductivity of NFs decreased by 3.0 and 1.8% at 25 °C for NFs composed of 2 wt % MWCNTs and 1,2-PG or 1,3-PG, respectively (see also Figure 3C,D and Tables S7 and S8). Thus, taking into consideration the uncertainty of the thermal conductivity measurements of ±5%, we can assume that the thermal conductivity did not change during 8 months, which is significant for the application of these types of systems. The carbon nanotubes provide high thermal conductivity due to the effective heat transport along relatively large distances in the order of micrometers. From the cryo-TEM data analysis, the existence of partial clustering and chain-like linear aggregation could be postulated (Figure 1E,F) that can explain the thermal conductivity enhancement. Additionally, from the cryo-TEM data, the effect of the formation of the interfacial layer characterized by higher thermal conductivity than that of the bulk phase[11] can be also observed (Figure 1C−F). The most likely phenomenon in the systems under study is the formation of the interfacial layer via adsorption of PVP on the CNT surface.

In practice, the trade-off between the heat transfer capabilities and viscosity of the HTFs is required. Low viscosity under operating conditions improves the medium's ability to exchange heat, thereby reducing the amount of power consumption by recirculating pumps and enabling systems to achieve lower minimum operating temperatures. The viscosity of pure propanediols was measured in the temperature range from −10 to 70 °C, while the viscosity of NFs composed of 2 wt % MWCNTs + 1,2-PG and 2 wt % MWCNTs + 1,3-PG was measured in the temperature range from 10 to 60 °C immediately after sonication. The experimental results are collected in Tables S9 and S10 in the Supporting Information and presented in Figure 4. 1,3-PG and 1,2-PG are constitutional isomers of different properties. Therefore, 1,3-PG has an improved viscosity profile at low temperatures as compared to 1,2-PG, that is, the viscosity is lower by 53% at −10 °C (Figure 4A). The viscosity of NFs was measured as a function of the shear rate at 25 °C. Regardless of the concentration of MWCNTs and the type of the base medium, the viscosity of NFs is practically independent of the shear rate in the range 20−100 s^{-1} (see also Figure 4C,D). Thus, the enhancement in thermal conductivity is accompanied by the practically pure Newtonian behavior of NFs under investigation. As a consequence of lower viscosity of pure 1,3-PG than that of 1,2-PG, the NFs based on 1,3-PG have lower viscosity than NFs based on 1,2-PG, and the viscosity of NFs increases linearly with the MWCNT loading (Figure 4B). The viscosity of pure 1,2-PG, 1,3-PG, and NFs decreases significantly with temperature (Figure 4E,F). This decline equals 87% for 1,2-PG and NFs composed of 2 wt % MWCNTs + 1,2-PG and 92% for 1,3-PG and NFs composed of 2 wt % MWCNTs + 1,3-PG in the temperature range from 10 to 60 °C. However, in the temperature range from −10 to 70 °C, the decline equals 97 and 99% for pure 1,2-PG and 1,3-PG, respectively.

The studied 1,2-PG and 1,3-PG samples can be treated as model systems with physicochemical properties similar to those of commercial HTFs such as DOWCAL 200 and DOWCAL N (see Table S11 in the Supporting Information). The DOWCAL 200 HTF is composed of 92 wt % 1,2-PG and 8 wt % inhibitors and water.[39] DOWCAL 200 is characterized by low oral toxicity, which makes it particularly suitable for heating, ventilating, and air conditioning systems, ground-source heat pumps, and solar panels. It can also be used for secondary cooling systems in recreational facilities such as ice rinks. DOWCAL N is composed of 95.5 wt % 1,2-PG and 4.5 wt % water and a special corrosion inhibitor package.[39] DOWCAL N is used in the food and beverage industry. The thermal conductivity of NFs composed of 2 wt % MWCNTs + 1,3-PG is higher by 30% than the thermal conductivity of DOWCAL 200 and by 13% than that of DOWCAL N at 20 °C

https://doi.org/10.1021/acssuschemeng.1c01944
ACS Sustainable Chem. Eng. 2021, 9, 7369−7378

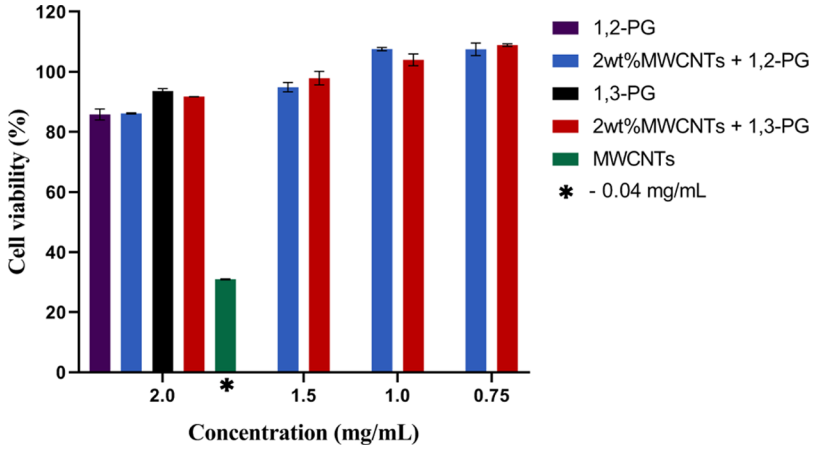

Figure 6. Dose-dependent viability of NHDF cells after 72 h incubation with the tested samples. *X*-axis represents the concentration of (i) fluids (1,2-PG and 1,3-PG), (ii) NFs containing 2 wt % MWCNTs, and (iii) pristine MWCNTs with an equal concentration of MWCNTs as that in the case of NFs—for comparative purposes—that is, 0.04 mg/mL.

(Figure 5). The molar isobaric heat capacity values of the selected NFs composed of 2 wt % MWCNTs + 1,2-PG and 2 wt % MWCNTs + 1,3-PG are higher than those of pure 1,2-PG and 1,3-PG by a maximum of 3.4 and 4.2%, respectively (see Tables S12 and S13 in the Supporting Information). The heat capacity is needed to estimate heating and cooling requirements as well as energy storage density as a product of the isobaric specific heat capacity and the density $C_p \cdot \rho$. The energy storage density is the most critical design parameter for working thermal fluids because a higher energy storage density results in a lower requirement for the thermal fluid volume. Typically, the energy storage density of the liquids is in the range 1.5−2.0 MJ·m^{-3}·K^{-1}.[40] The obtained results show that studied systems are characterized by a higher energy storage density, that is, 2.6−2.7 MJ·m^{-3}·K^{-1} for 1,2-PG; 2.7−2.8 MJ·m^{-3}·K^{-1} for 2 wt % MWCNTs + 1,2-PG; 2.4−2.5 MJ·m^{-3}·K^{-1} for 1,3-PG; and 2.5−2.7 MJ·m^{-3}·K^{-1} for 2 wt % MWCNTs + 1,3-PG, in the temperature range from 20 to 45 °C. These are similar values to the energy storage densities of DOWCAL 200 and DOWCAL N, which equal 2.3 and 2.6 MJ·m^{-3}·K^{-1} at 20 °C, respectively.[39] The ratio of the thermal conductivity and energy storage density yields thermal diffusivity $\alpha = k(C_p \times \rho)^{-1}$. For the investigated samples, the change in thermal diffusivity was determined by the change in thermal conductivity (please compare the appropriate Tables S7, S8, S12, and S13 in the Supporting Information). All of the most important parameters of HTFs consider the Prandtl number, *Pr*, which is the ratio of the isobaric heat capacity multiplied by the viscosity to the thermal conductivity, $Pr = C_p \cdot \eta/\lambda$. Nearly all of the variations in the Prandtl number are determined by the effect of temperature on viscosity. Values of the Prandtl number of NFs composed of 2 wt % MWCNTs + 1,2-PG or 1,3-PG are higher than those of pure diols and commercial HTFs DOWCAL 200 or DOWCAL N (Figure 5). These values are typical for oils and demonstrate that convective heat transfer is the dominating mechanism.[41]

MWCNTs owe their popularity in the nanotechnology to a superb combination of physicochemical and biological properties.[42] Scalability of CNT-based solutions for everyday life requires safety as the sine qua non.[43] However, there are numerous and frequently controversial studies concerning *in vitro* and *in vivo* toxicity studies on CNTs.[44] On the other hand, the bulk of aspects governing the CNT cytotoxicity was identified and classified. The key parameters include the chemical structure and composition, number and crystallinity/perfection of walls, dimension distribution (uniformity of the sample and aspect ratios), endo-/exohedral functionalization, surface charge, surface area, agglomeration versus individualization state, and presence of extraneous materials (catalyst particles and contaminations from the manufacturing processes), with all these factors being both time- and dose-dependent.[45] Accordingly, from the cell line perspective, it is the cell type and morphology which constitute the second equally important system for *in vivo* studies.[46] One of the most important problem upon testing the cytotoxicity of CNTs and CNT-based systems is insolubility in water, while, clearly, living cells function solely in the aqueous environments. Toward the initial evaluation of biosafety of the specific sample of the MWCNT system we deal with, that is, composed of PVP- (as the surfactant) and short-nanotube-individualized longer nanotubes in glycols (please refer back to Figure 1), we decided to perform the *in vitro* cytotoxic assays for NHDF cells. The rationale behind such a selection was twofold. First, the skin is potentially the most vulnerable tissue to the potential bio-based NFs. Second, the immobilization of MWCNTs in the liquid phase practically eliminates other routes of exposure. Typically, to minimize the effects of various dispersibilities of nanomaterials, the appropriate sample is dissolved in the culture medium or in a small amount (0.3%) of DMSO and then in the medium.

Here, we prepared the MWCNT dispersions in the absence of DMSO, administered to the cells and incubated at the appropriate time. For comparison, only a concentration as small as 0.04 mg/mL was achievable by dispersing pure MWCNTs in the medium. The pure 1,2-PG and 1,3-PG samples were dissolved in a culture medium in a high concentration (20 mg/mL) and after 72 h of the incubation with NHDF cell line did not inhibit the proliferation of cells. After dispersion of NFs composed of 2 wt % MWCNTs and 1,2-PG or 1,3-PG in a medium containing BSA, we have received systems at a concentration of 2 mg/mL sufficiently dispersible to test their cytotoxicity. The maximal concentration achieved did not cause an inhibition of the proliferation of the tested cell line. These results are important from two points of view: (i) NFs are considerably better dispersible in the medium than the pure MWCNT, and (ii) at 2 mg/mL, the

https://doi.org/10.1021/acssuschemeng.1c01944
ACS Sustainable Chem. Eng. 2021, 9, 7369−7378

formulations of NFs composed of 2 wt % MWCNTs and 1,2-PG or 1,3-PG were practically of the same cytotoxicity as the base fluids and of insignificant overall toxicity toward normal dermal fibroblasts. MWCNTs alone, at 0.04 mg/mL, inhibited the proliferation of cells to 30% (Figure 6). At the same time, when MWCNTs were dispersed in diols at the identical concentration (0.04 mg/mL), the samples did not show a toxic effect. These results indicate that the juxtaposition of the diols with MWCNTs diminishes the toxicity of the latter—due to more extensive MWCNT individualization and hence enhanced dispersibility. It should be emphasized that our findings stay in line with the studies by Canapè et al. (l = 200−400 nm) on PEG10000-coated MWCNTs where a similar cytotoxicity though during a shorter, that is, 24 h, exposure was found.[47] Also, Patlolla et al. studied the cytotoxicity of MWCNTs against NHDF and found that significantly longer, that is, 12 μm long, MWCNTs led to a ca. 30% higher increase in the population of apoptotic and necrotic cells as compared to our results.[48] The authors assigned this behavior to the nanotube morphology. Indeed, individualization- and hydrophilization-driven dispersibility of MWCNTs toward lower hydrodynamic radii might actually lead to the complete alleviation of their intrinsic toxicity.[49] Here, PVP and short nanotubes should yield identical but, in fact, synergetic effects.

CONCLUSIONS

The addition of the MWCNTs into 1,2-PG and 1,3-PG as well as stabilization with PVP, which is a rare case for carbon-based NFs, leads to enhancements in thermal conductivity of 22 and 20% for NFs composed of 2 wt % MWCNTs in comparison with that of pure 1,2-PG and 1,3-PG, respectively. Importantly, this figure is accompanied by (i) a practically pure Newtonian character under a range of shear rates and (ii) long-term, that is, more than 1 year (14 months), sedimentation stability at high MWCNT concentrations. The real image of NFs determined by the unique cryo-TEM method showed fully individualized MWCNTs in the continuous phase and MWCNTs stabilized in dispersions by shorter, amorphous elongated/ellipsoidal or spheroidal carbon nanoparticles and mostly homogenous PVP coating. Moreover, the use of diols diminishes the *in vitro* cytotoxicity of the MWCNTs against healthy cell lines, that is, normal human dermal fibroblasts. Finally, the thermal conductivity of NFs composed of 2 wt % MWCNTs + 1,3-PG is higher by 30% than the thermal conductivity of DOWCAL 200 and by 13% than that of DOWCAL N at 20 °C. Thus, we composed bio-based NFs with many advantageous properties, which predestine them as not only reliable but also superb green heat transfer media in the sustainable energy systems. This is indeed already reflected in the interest of the industry, and the results of this collaboration will be the subject of our studies in the very near future. Additionally, we plan to apply in-house MWCNTs with the extreme values of the length-to-diameter ratio (aspect ratio) of 11,000 in order to substantially improve the thermal conductivity of PG-based NFs.

ASSOCIATED CONTENT

Supporting Information

The Supporting Information is available free of charge at https://pubs.acs.org/doi/10.1021/acssuschemeng.1c01944.

Specification of propanediols, results of thermal conductivity test measurements, density of NFs, thermal conductivity of NFs, viscosity of NFs, properties of 1,2-PG, 1,3-PG, and commercial HTFs DOWCAL 200 and DOWCAL N, specific isobaric heat capacity of NFs, and thermal diffusivity of NFs (PDF)

AUTHOR INFORMATION

Corresponding Authors

Karolina Brzóska − *University of Silesia in Katowice, Institute of Chemistry, Katowice 40-006, Poland; Boryszew S.A. Branch Boryszew ERG Sochaczew, Sochaczew 96-500, Poland*; Email: kbrzoska@us.edu.pl

Sławomir Boncel − *Department of Organic Chemistry, Bioorganic Chemistry and Biotechnology, Silesian University of Technology, Gliwice 44-100, Poland*; orcid.org/0000-0002-0787-5243; Email: slawomir.boncel@polsl.pl

Marzena Dzida − *University of Silesia in Katowice, Institute of Chemistry, Katowice 40-006, Poland*; orcid.org/0000-0001-9566-4093; Email: marzena.dzida@us.edu.pl

Authors

Adrian Golba − *University of Silesia in Katowice, Institute of Chemistry, Katowice 40-006, Poland*

Michał Kuczak − *University of Silesia in Katowice, Institute of Chemistry, Katowice 40-006, Poland; A. Chełkowski Institute of Physics and Silesian Center for Education and Interdisciplinary Research, University of Silesia in Katowice, Chorzów 41-500, Poland*

Anna Mrozek-Wilczkiewicz − *A. Chełkowski Institute of Physics and Silesian Center for Education and Interdisciplinary Research, University of Silesia in Katowice, Chorzów 41-500, Poland*

Complete contact information is available at: https://pubs.acs.org/10.1021/acssuschemeng.1c01944

Notes

The authors declare no competing financial interest.

ACKNOWLEDGMENTS

A.G., S.B., and M.D. thank the National Science Centre (Poland) for the financial support in the framework of OPUS grant no. 2017/27/B/ST4/02748. The authors are profoundly indebted to Paweł Gancarz, MSc, for isobaric heat capacity test measurements.

REFERENCES

(1) Samudrala, S. P.; Kandasamy, S.; Bhattacharya, S. Turning Biodiesel Waste Glycerol into 1,3-Propanediol: Catalytic Performance of Sulphuric acid-Activated Montmorillonite Supported Platinum Catalysts in Glycerol Hydrogenolysis. *Sci. Rep.* **2018**, *8*, 7484.

(2) Ju, J.-H.; Wang, D.; Heo, S.-Y.; Kim, M.-S.; Seo, J.-W.; Kim, Y.-M.; Kim, D.-H.; Kang, S.-A.; Kim, C.-H.; Oh, B.-R. Enhancement of 1,3-propanediol production from industrial by-product by Lactobacillus reuteri CH53. *Microb. Cell Factories* **2020**, *19*, 6.

(3) https://secureservercdn.net/198.71.233.47/6hh.09f.myftpupload.com/wp-content/uploads/Susterra_Brochure_Low_Temperature_Heat_Transfer_2017.pdf (access 19 March 2021).

(4) Gómez-Jiménez-Aberasturi, O.; Ochoa-Gómez, J. R. New approaches to producing polyols from biomass. *J. Chem. Technol. Biotechnol.* **2017**, *92*, 705−711.

(5) https://secureservercdn.net/198.71.233.47/6hh.09f.myftpupload.com/wp-content/uploads/Susterra_for_high_temperature_glycol_fluids_2016.pdf (access 19 March 2021).

(6) Sekrani, G.; Poncet, S. Ethylene- and Propylene-Glycol Based Nanofluids: A Litterature Review on Their Thermophysical Properties and Thermal Performances. *Appl. Sci.* **2018**, *8*, 2311.
(7) LaKind, J. S.; McKenna, E. A.; Hubner, R. P.; Tardiff, R. G. A Review of the Comparative Mammalian Toxicity of Ethylene Glycol and Propylene Glycol. *Crit. Rev. Toxicol.* **1999**, *29*, 331−365.
(8) Xie, H.; Lee, H.; Youn, W.; Choi, M. Nanofluids containing multiwalled carbon nanotubes and their enhanced thermal conductivities. *J. Appl. Phys.* **2003**, *94*, 4967−4971.
(9) Liu, M.-S.; Ching-Cheng Lin, M.; Huang, I.-T.; Wang, C.-C. Enhancement of Thermal Conductivity with Carbon Nanotube for Nanofluids. *Int. Commun. Heat Mass Tran.* **2005**, *32*, 1202−1210.
(10) de Castro, C. A. N.; Murshed, S. M. S.; Lourenço, M. J. V.; Santos, F. J. V.; Lopes, M. L. M.; França, J. M. P. Ionanofluids: New Heat Transfer Fluids for Green Processes Development. In *Green Solvents I*; Inamuddin, M. A., Ed.; Springer: Dordrecht, the Netherlands, 2012, pp 233−249. DOI: 10.1007/978-94-007-1712-1_8.
(11) Jóźwiak, B.; Dzido, G.; Zorębski, E.; Kolanowska, A.; Jędrysiak, R.; Dziadosz, J.; Libera, M.; Boncel, S.; Dzida, M. Remarkable Thermal Conductivity Enhancement in Carbon-Based Ionanofluids: Effect of Nanoparticle Morphology. *ACS Appl. Mater. Interfaces* **2020**, *12*, 38113−38123.
(12) Boncel, S.; Zniszczoł, A.; Pawlyta, M.; Labisz, K.; Dzido, G. Heat transfer nanofluid based on curly ultra-long multi-wall carbon nanotubes. *Heat Mass Tran.* **2018**, *54*, 333−339.
(13) Mary, A. H.; Suganthi, K. S.; Rajan, K. S. Mechanistic Investigations of Viscosity and Thermal Conductivity Enhancement in Multi-Walled Carbon Nanotubes-Propylene Glycol Nanofluids. *Nanosci. Nanotechnol. Lett.* **2013**, *5*, 1125−1129.
(14) Bhattacharya, K.; Mukherjee, S. P.; Gallud, A.; Burkert, S. C.; Bistarelli, S.; Bellucci, S.; Bottini, M.; Star, A.; Fadeel, B. Biological Interactions of Carbon-Based Nanomaterials: From Coronation to Degradation. *Nanomedicine* **2016**, *12*, 333−351.
(15) Kagan, V. E.; Kapralov, A. A.; St. Croix, C. M.; Watkins, S. C.; Kisin, E. R.; Kotchey, G. P.; Balasubramanian, K.; Vlasova, I. I.; Yu, J.; Kim, K.; Seo, W.; Mallampalli, R. K.; Star, A.; Shvedova, A. A. Lung Macrophages "Digest" Carbon Nanotubes Using a Superoxide/Peroxynitrite Oxidative Pathway. *ACS Nano* **2014**, *8*, 5610−5621.
(16) Kotchey, G. P.; Zhao, Y.; Kagan, V. E.; Star, A. Peroxidase-mediated biodegradation of carbon nanotubes in vitro and in vivo. *Adv. Drug Delivery Rev.* **2013**, *65*, 1921−1932.
(17) Zhao, Y.; Allen, B. L.; Star, A. Enzymatic Degradation of Multiwalled Carbon Nanotubes. *J. Phys. Chem. A* **2011**, *115*, 9536−9544.
(18) Zorębski, E.; Dzida, M.; Piotrowska, M. Study of the Acoustic and Thermodynamic Properties of 1,2- and 1,3-Propanediol by Means of High-Pressure Speed of Sound Measurements at Temperatures from (293 to 318) K and Pressures up to 101 MPa. *J. Chem. Eng. Data* **2008**, *53*, 136−144.
(19) Bajić, D. M.; Živović, E. M.; Šerbanović, S. P.; Kijevčanin, M. L. Experimental measurements and modelling of volumetric properties, refractive index and viscosity of selected binary systems with butyl lactate at 288.15−323.15K and atmospheric pressure. New UNIFAC-VISCO interaction parameters. *Thermochim. Acta* **2013**, *562*, 42−55.
(20) Arce, A.; Marchiaro, A.; Soto, A. Propanediols for separation of citrus oil: liquid-liquid equilibria of limonene + linalool + (1,2-propanediol or 1,3-propanediol). *Fluid Phase Equilib.* **2003**, *211*, 129−140.
(21) George, J.; Sastry, N. V. Densities, Dynamic Viscosities, Speeds of Sound, and Relative Permittivities for Water + Alkanediols (Propane-1,2- and -1,3-diol and Butane-1,2-, -1,3-, -1,4-, and -2,3-Diol) at Different Temperatures. *J. Chem. Eng. Data* **2003**, *48*, 1529−1539.
(22) Deng, C.; Zhang, K. Thermal Conductivity of 1,2-Ethanediol and 1,2-Propanediol Binary Aqueous Solutions at Temperature from 253 K to 373 K. *Int. J. Thermophys.* **2021**, *42*, 81.
(23) Vargaftik, N. B. *Handbook of Thermal Conductivity of Liquids and Gases*; CRC Press, Taylor & Francis, 1993.
(24) Mallan, G. M.; Michaelian, M. S.; Lockhart, F. J. Liquid Thermal Conductivities of Organic Compounds and Petroleum Fractions. *J. Chem. Eng. Data* **1972**, *17*, 412−415.
(25) Hemmat, M.; Moosavi, M.; Rostami, A. A. Study on volumetric and viscometric properties of 1,4-Dioxane and 1,2-Ethanediol/1,3-Propanediol binary liquid mixtures, measurement and prediction. *J. Mol. Liq.* **2017**, *225*, 107−117.
(26) Bleazard, J. G.; Sun, T. F.; Johnson, R. D.; DiGuillio, R. M.; Teja, A. S. The Transport Properties of Seven Alkanediols. *Fluid Phase Equilib.* **1996**, *117*, 386−393.
(27) ASTM D7896 - 19 Standard Test Method for Thermal Conductivity, Thermal Diffusivity, and Volumetric Heat Capacity of Engine Coolants and Related Fluids by Transient Hot Wire Liquid Thermal Conductivity Method.
(28) Ramires, M. L. V.; Nieto de Castro, C. A.; Nagasaka, Y.; Nagashima, A.; Assael, M. J.; Wakeham, W. A. Standard Reference Data for the Thermal Conductivity of Water. *J. Phys. Chem. Ref. Data* **1995**, *24*, 1377−1381.
(29) França, J. M. P.; Vieira, S. I. C.; Lourenço, M. J. V.; Murshed, S. M. S.; Nieto de Castro, C. A. Thermal Conductivity of [C4mim][(CF3SO2)2N] and [C2mim][EtSO4] and Their IoNanofluids with Carbon Nanotubes: Experiment and Theory. *J. Chem. Eng. Data* **2013**, *58*, 467−476.
(30) Ramires, M. L. V.; Nieto de Castro, C. A.; Perkins, R. A.; Nagasaka, Y.; Nagashima, A.; Assael, M. J.; Wakeham, W. A. Reference Data for the Thermal Conductivity of Saturated Liquid Toluene Over a Wide Range of Temperatures. *J. Phys. Chem. Ref. Data* **2000**, *29*, 133−139.
(31) Nieto de Castro, C. A.; Li, S. F. Y.; Nagashima, A.; Trengove, R. D.; Wakeham, W. A. Standard Reference Data for the Thermal Conductivity of Liquids. *J. Phys. Chem. Ref. Data* **1986**, *15*, 1073−1086.
(32) Ogiwara, K.; Arai, Y.; Saito, S. Thermal conductivities of liquid alcohols and their binary mixtures. *J. Chem. Eng. Jpn.* **1982**, *15*, 335−342.
(33) Raal, J. D.; Rijsdijk, R. L. Measurement of Alcohol Thermal Conductivities Using a Relative Strain-Compensated Hot-wire Method. *J. Chem. Eng. Data* **1981**, *26*, 351−359.
(34) Brzóska, K.; Jóźwiak, B.; Golba, A.; Dzida, M.; Boncel, S. Thermophysical Properties of Nanofluids Composed of Ethylene Glycol and Long Multi-Walled Carbon Nanotubes. *Fluids* **2020**, *5*, 241.
(35) Bogacheva, I. S.; Zemdikhanov, K. B.; Mukhamedzyanov, G. Kh.; Sadykov, A. Kh.; Usmanov, A. G. Heat Conductivity of Mixtures of Organic Liquids. *Zh. Fiz. Khim.* **1980**, *54*, 1468−1470. (in Russian)
(36) Herman, A. P.; Boncel, S. Oxidised carbon nanotubes as dual-domain synergetic stabilizers in electroconductive carbon nanotube flexible coatings. *RSC Adv.* **2018**, *8*, 30712−30716.
(37) Heister, E.; Lamprecht, C.; Neves, V.; Tîlmaciu, C.; Datas, L.; Flahaut, E.; Soula, B.; Hinterdorfer, P.; Coley, H. M.; Silva, S. R. P.; McFadden, J. Higher Dispersion Efficacy of Functionalized Carbon Nanotubes in Chemical and Biological Environments. *ACS Nano* **2010**, *4*, 2615−2626.
(38) Ntim, S. A.; Sae-Khow, O.; Witzmann, F. A.; Mitra, S. Effects of polymer wrapping and covalent functionalization on the stability of MWCNT in aqueous dispersions. *J. Colloid Interface Sci.* **2011**, *355*, 383−388.
(39) DOWCAL Fluids Inhibited Glycol-based Heat Transfer Fluids, Guide to Products, System Design, Installation and Operation (access 19 March, 2021). https://www.dow.com/content/dam/dcc/documents/en-us/mark-prod-info/180/180-01455-01-dowcal-inhibited-glycolbased-heat-transfer-fluids.pdf.
(40) Holbrey, J. D.; Reichert, W. M.; Reddy, R. G.; Rogers, R. D. Heat Capacities of Ionic Liquids and their Applications as Thermal Fluids. *ACS Symposium Series 856 Ionic Liquids as Green Solvents*, 2003; Vol. *11*; pp 121−133.
(41) Tenney, C. M.; Massel, M.; Mayes, J. M.; Sen, M.; Brennecke, J. F.; Maginn, E. J. A Computational and Experimental Study of the

Heat Transfer Properties of Nine Different Ionic Liquids. *J. Chem. Eng. Data* **2014**, *59*, 391−399.
(42) De Volder, M. F. L.; Tawfick, S. H.; Baughman, R. H.; Hart, A. J. Carbon Nanotubes: Present and Future Commercial Applications. *Science* **2013**, *339*, 535−539.
(43) Sousa, S. P. B.; Peixoto, T.; Santos, R. M.; Lopes, A.; Paiva, M. d. C.; Marques, A. T. Health and Safety Concerns Related to CNT and Graphene Products, and Related Composites. *J. Compos. Sci.* **2020**, *4*, 106.
(44) Heller, D. A.; Jena, P. V.; Pasquali, M.; Kostarelos, K.; Delogu, L. G.; Meidl, R. E.; Rotkin, S. V.; Scheinberg, D. A.; Schwartz, R. E.; Terrones, M.; Wang, Y.; Bianco, A.; Boghossian, A. A.; Cambré, S.; Cognet, L.; Corrie, S. R.; Demokritou, P.; Giordani, S.; Hertel, T.; Ignatova, T.; Islam, M. F.; Iverson, N. M.; Jagota, A.; Janas, D.; Kono, J.; Kruss, S.; Landry, M. P.; Li, Y.; Martel, R.; Maruyama, S.; Naumov, A. V.; Prato, M.; Quinn, S. J.; Roxbury, D.; Strano, M. S.; Tour, J. M.; Weisman, R. B.; Wenseleers, W.; Yudasaka, M. Banning carbon nanotubes would be scientifically unjustified and damaging to innovation. *Nat. Nanotechnol.* **2020**, *15*, 164−166.
(45) Devadasu, V. R.; Bhardwaj, V.; Kumar, M. N. V. R. Can controversial nanotechnology promise drug delivery? *Chem. Rev.* **2013**, *113*, 1686−1735.
(46) Boncel, S.; Pluta, A.; Skonieczna, M.; Gondela, A.; Maciejewska, B.; Herman, A. P.; Jędrysiak, R. G.; Budniok, S.; Komędera, K.; Błachowski, A.; Walczak, K. Z. Hybrids of Iron-Filled Multiwall Carbon Nanotubes and Anticancer Agents as Potential Magnetic Drug Delivery Systems: In Vitro Studies against Human Melanoma, Colon Carcinoma, and Colon Adenocarcinoma. *J. Nanomater.* **2017**, *2017*, 1.
(47) Canapè, C.; Foillard, S.; Bonafè, R.; Maiocchi, A.; Doris, E. Comparative assessment of the in vitro toxicity of some functionalized carbon nanotubes and fullerenes. *RSC Adv.* **2015**, *5*, 68446.
(48) Patlolla, A.; Knighten, B.; Tchounwou, P. Multi-walled carbon nanotubes induce cytotoxicity, genotoxicity and apoptosis in normal human dermal fibroblast cells. *Ethn. Dis.* **2010**, *20*, S1−65. PMCID PMC2902968
(49) Ali-Boucetta, H.; Nunes, A.; Sainz, R.; Herrero, M. A.; Tian, B.; Prato, M.; Bianco, A.; Kostarelos, K. Asbestos-like Pathogenicity of Long Carbon Nanotubes Alleviated by Chemical Functionalization. *Angew. Chem., Int. Ed.* **2013**, *52*, 2274−2278.

https://doi.org/10.1021/acssuschemeng.1c01944
ACS Sustainable Chem. Eng. 2021, 9, 7369−7378